2. Watanabe N, Ogasawara Y, Yamaura Y, et al. Quantitation of mitral valve tenting in ischemic mitral regurgitation by transthoracic real-time three-dimensional echocardiography. J Am Coll Cardiol 2005; 45:763–9.
3. Delgado V, Tops LF, Schuijf JD, et al. Assessment of mitral valve anatomy and geometry with multislice computed tomography. J Am Coll Cardiol Img 2009;2:556–65.
4. Kaji S, Nasu M, Yamamuro A, et al. Annular geometry in patients with chronic ischemic mitral regurgitation: three-dimensional magnetic resonance imaging study. Circulation 2005;112:I409–14.

▶APPENDIX

For MSCT protocols and 3D measurements, supplementary figures 1 and 2, and a supplementary table, please see the online version of this article.

OCT-Verified Neointimal Hyperplasia Is Increased at Fracture Site in Drug-Eluting Stents

Although drug-eluting stents dramatically reduce stent restenosis, in-stent restenosis still occurs in approximately 10% of sirolimus-eluting stent (SES) implantation cases. Optical coherence tomography (OCT) has the potential to assess neointima hyperplasia precisely in vivo (1). However, the morphological features of stent fracture in OCT imaging have not yet been reported, and there is no OCT study that clarifies the relationship between stent fracture and neointimal hyperplasia in SES. We investigated the morphological features of stent fracture in OCT to clarify the relationship between stent fracture and neointimal hyperplasia in SES.

We enrolled 110 adequately expanded SES (BxVelocity platform) stents from 70 patients. For overlapped stents (n = 41), we confirmed complete overlapping in the post-procedural angiography. The scheduled coronary angiography and OCT imaging were performed at 11 ± 6 months after SES implantation. According to the presence of stent fracture in breath-hold fluoroscopy, stents were divided into a fractured stent group and a nonfractured stent group. Binary restenosis was defined as a >50% stenosis by the CMS-QCA system (CMS-MEDIS, Medical Imaging Systems, Leiden, the Netherlands). An OCT 0.016-inch catheter (ImageWire, LightLab Imaging, Westford, Massachusetts) was used, and all OCT image acquisitions were performed with the continuous-flushing method (2). To coregister OCT images and coronary angiograms on an individual stent basis, we used the distance from each stent edge, the tip of guiding catheter, and anatomical landmarks. Stent area, lumen area, and neointima area were measured according to a previous report (3). In case stent struts cannot be recognized, substitute stent area, which was an average stent area of both broken edges of the fractured stent, was applied (Fig. 1). Neointimal area was assessed in multiple slices, incrementally spaced by 1 mm from fracture site to distal and proximal sites. To assess the distribution pattern of neointima within the stent, neointimal hyperplasia was repartitioned along the stent length into 18 segments.

Stent fracture was observed in 14 (12.7%) of 110 stents. The fractured stent group showed higher binary in-stent restenosis (29% vs. 6%, p = 0.02) and percent diameter stenosis (44.8 ±

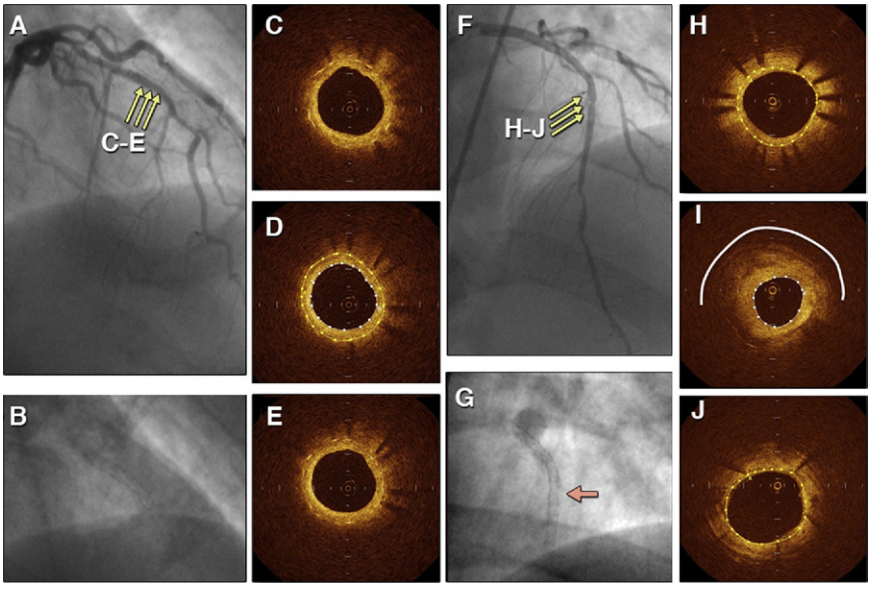

Figure 1. An Exactly Matching Set Among Angiography, Fluoroscopy, and OCT

A nonfractured stent shows **(A)** no restenosis in angiography, **(B)** no distorted stent in fluoroscopy, **(C)** preserved coronary lumen **(white circle)**, and **(D)** well-covered stent struts **(yellow circle)** in optical coherence tomography (OCT). **(C–E)** Neointima grows evenly. A fractured stent shows **(F)** focal restenosis in angiography, **(G)** distorted and fractured stent in fluoroscopy, and **(I)** excessive neointimal hyperplasia with absence of stent struts **(white line)** at fractured site in OCT. **(H, J)** A substitute stent area that is the average stent area of both broken edges of the fractured stent **(yellow circle)** is applied for neointimal area assessment at fractured site.

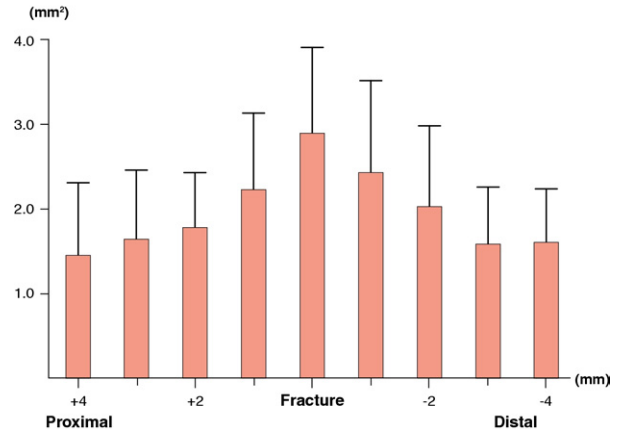

Figure 2. Neointimal Hyperplasia Area and Distance From the Fracture Site

The distribution of neointimal hyperplasia shows a peak at the fracture site. Data are shown as mean with SD.

28.0% vs. 14.9 ± 23.6%, $p < 0.01$) compared with the nonfractured stent group. The absence of stent strut was the common morphological feature of stent fracture in OCT. Both mean and maximal neointimal area were larger in the stent fracture group (fracture 1.59 ± 0.75 mm^2 vs. nonfracture 0.55 ± 0.46 mm^2, $p < 0.01$; and fracture 3.30 ± 1.73 mm^2 vs. nonfracture 1.28 ± 1.10 mm^2, $p < 0.01$, respectively). Although neointima grew equally in the nonfractured stent group, the distribution of neointimal area showed a peak at the fracture site in the fractured stent group (Fig. 2). The longitudinal length of the absence of stent struts was positively correlated with the neointimal area at the fracture site ($r = 0.79$, $p < 0.01$). From the receiver-operating characteristics curve, the best cutoff value of the length of the absence of stent struts to diagnose stent fracture was 1.07 mm (area under the curve 0.85, sensitivity 93%, and specificity 80%).

The absence of stent strut was the common morphological feature of stent fracture, and its length was correlated with the neointimal area. These results suggest that the loss of stent strut itself is one of the important contributors to excessive neointimal growth. Previous ex vivo studies reported that cyclic stretch on cultured cells induces the proliferation of vascular smooth muscle cells. We have reported that stent fracture frequently occurs at bend lesions (4). When stent fracture occurs, the stent loses its ability to scaffold the artery wall against mechanical stress. We speculate that occurrence of these mechanical stresses at the fracture site could contribute to excessive neointimal growth. Furthermore, many previous studies have postulated other causes for SES restenosis including stent under-expansion, polymer disruption, stent strut inconsistent distribution, and stent fracture. These factors could directly or indirectly affect the drug delivery. Even though it is difficult to know when the stent was fractured, we speculate that a loss of stent struts at the fracture site may impede effective local drug delivery, resulting in failure to prevent the neointimal growth.

This study has several limitations. We only analyzed a small number of fractured stents. Fluoroscopy might miss small stent fractures because of its low spatial resolution. Thrombus or lipid components may disturb the accurate assessment of neointima area. There is also a possibility that stent struts covered with thick neointima may be misdiagnosed as the disappearance of stent struts. In conclusion, OCT could diagnose stent fracture, and neointimal hyperplasia is enhanced at the fracture site.

Manabu Kashiwagi, MD, Atsushi Tanaka, MD,*
Hironori Kitabata, MD, Yasushi Ino, MD, Hiroto Tsujioka, MD,
Kenichi Komukai, MD, Yuichi Ozaki, MD, Kohei Ishibashi, MD,
Takashi Tanimoto, MD, Shigeho Takarada, MD,
Takashi Kubo, MD, Kumiko Hirata, MD,
Masato Mizukoshi, MD, Toshio Imanishi, MD,
Takashi Akasaka, MD

*Department of Cardiovascular Medicine, Wakayama Medical University, 811-1 Kimiidera, Wakayama 641-8509, Japan.
E-mail: a-tanaka@wakayama-med.ac.jp

doi:10.1016/j.jcmg.2011.07.014

REFERENCES

1. Suzuki Y, Ikeno F, Koizumi T, et al. In vivo comparison between optical coherence tomography and intravascular ultrasound for detecting small degrees of in-stent neointima after stent implantation. J Am Coll Cardiol Intv 2008;1:168–73.
2. Tanaka A, Imanishi T, Kitabata H, et al. Morphology of exertion-triggered plaque rupture in patients with acute coronary syndrome: an optical coherence tomography study. Circulation 2008;118:2368–73.
3. Murata A, Wallace-Bradley D, Tellez A, et al. Accuracy of optical coherence tomography in the evaluation of neointimal coverage after stent implantation. J Am Coll Cardiol Img 2010;3:76–84.
4. Ino Y, Toyoda Y, Tanaka A, et al. Predictors and prognosis of stent fracture after sirolimus-eluting stent implantation. Circ J 2009;73:2036–41.

T_2-Weighted CMR

But Where Is Elvis in the End?

A few months ago, in an editorial by Raman et al. (1), T_2-weighted (T_2w) short tau inversion recovery (STIR) imaging, the only validated T_2 sequence that was tested against pathology in an experimental setting to assess the myocardial area at risk (AAR), was almost thrown out the window because of its limited accuracy and poor reproducibility due to the high sensitivity to artifacts. However, there was still hope, because better sequences have come out (T_2w ACUTE [Acquisition for Cardiac Unified T2 Edema], T_2prep steady-state free precession, T_2 mapping) with significantly better reproducibility and accuracy. But those sequences have not been validated against pathology.

In a recent issue of *iJACC*, Fuernau and Eitel et al. (2) have published successively several papers about large groups of acute ST-segment elevation myocardial infarction patients in whom T_2wSTIR was used to assess the AAR. Their results showed that T_2wSTIR had a significant prognostic value, and it was well correlated to angiographic surrogates of the myocardial AAR. At